Systematics in the structure of low-lying, nonyrast bandhead configurations of strongly deformed nuclei

G. Popa,[1,*] A. Georgieva,[2,3] and J. P. Draayer[3]
[1]*Department of Physics, Rochester Institute of Technology, Rochester, New York 14623, USA*
[2]*INRNE, Bulgarian Academy of Science, Sofia, 1784 Bulgaria*
[3]*Department of Physics and Astronomy, Louisiana State University, Baton Rouge, Louisiana 70803, USA*
(Received 20 October 2003; published 7 June 2004)

An empirical investigation of the trends in the properties of the nonyrast $K^\pi=2^+_\gamma$ and $K^\pi=0^+_2$ bandhead configurations in nuclei that are related to one another through the addition or removal of α-particle-like structures, reveals their complex and changing behavior in contrast to the smooth behavior of the yrast states. A systematic application of the pseudo-SU(3) model for such a sequence of deformed nuclei from the rare earth region leads to an accurate and unified description of not only yrast, but nonyrast collective bands. The onset of deformation as manifested through the position of the excited bandheads in the spectra is understood and interpreted by using a realistic model Hamiltonian in conjunction with a microscopic distribution of the eigenstates across allowed proton and neutron strong-coupled SU(3) configurations.

DOI: 10.1103/PhysRevC.69.064307 PACS number(s): 21.60.Fw, 21.10.Re, 27.70.+q

I. INTRODUCTION

Various features of low-lying levels of even-even atomic nuclei can be used to test collective models of nuclear structure. The assumptions that go into the development of such models usually are based first on understanding the structure of states that belong to the ground-state band (g.s.b.), and then on properties of the excited bands, including especially the excitation energies of the bandhead configurations. This can lead to different interpretations of the same features of the spectra. An example is the behavior of the bands built on the lowest excited 0^+ and 2^+ states in well-deformed nuclei [1]. The properties of these levels are usually defined and interpreted within the framework of a geometrical approach to nuclear structure as bandheads of β and γ bands that arise out of the quadrupole surface vibrations of a deformed liquid drop [2,3]. With the development of new experimental techniques and the accumulation of additional data, various new and more refined models have been introduced in order to interpret and describe the ever growing volume of results [4]. A close systematic investigation into the properties of many low-lying, nonyrast states reveals that there are large differences in the observed data, even for neighboring nuclides. One can find many examples to support various interpretations of these configurations, which we will label by $K^\pi=0^+_2=0^+_\beta$ (second excited 0^+ state or the bandhead of the β band) and $K^\pi=2^+_\gamma$ (which may or may not be the second excited 2^+ state). The seemingly complex and changing behavior of the lowest excited nonyrast bands calls for a deeper understanding of their microscopic structure.

The unified treatment of a large amount of nuclear structure data is normally based on a systematic consideration of the properties of the systems being studied. Here we review systematics in the structure of key levels (bandheads of the γ and β bands relative to that of the ground state) in the low-energy spectra of a series of heavy deformed nuclei that differ from one another by α-particle-like structures. Such an approach has been tested empirically and shown to be convenient for a unified description of the low-lying yrast energies of the even-even nuclei [5,6]. The $K^\pi=0^+_2$ (β) and $K^\pi=2^+_\gamma$ (γ) bandheads show some rather sharp oscillations, in contrast with the smooth and periodic behavior of the yrast bandhead configuration, especially in regions with clearly observed rotational bands. Consequently, it is a challenging task to study trends in this behavior and offer an interpretation that reproduces the observations so one can make reliable predictions regarding newly obtained data or the structure of yet-to-be explored systems.

To interpret and reproduce properties of the low-lying spectra of deformed even-even nuclei, we apply a proton-neutron version of the pseudo-SU(3) shell model [7]. This scheme is particularly useful since it combines a consideration of the microscopic structure of nuclei with simple but general symmetry principles. Specifically, the pseudo-SU(3) model has been shown to be appropriate for a description of the low-lying spectra of the strongly deformed nuclei [8–10]. Another advantage of this approach is that it gives a geometrical interpretation of many-nucleon states through an established relationship between the SU(3) invariants and the shape variables β and γ of the geometrical collective model [11].

II. EMPIRICAL INVESTIGATION OF THE $K^\pi=0^+_2$ AND 2^+_γ BANDHEADS

Through an empirical investigation of yrast state energies of all even-even nuclei [5], the authors identified a unified theoretical description by superimposing a classification scheme that links species within major valence shell sets. This classification scheme depends only on two numbers, the total number of valence bosons $N=N_\pi+N_\nu$ and the third pro-

*On leave from the National Institute for Physics and Nuclear Engineering Horia Hulubei, Bucharest, Romania.

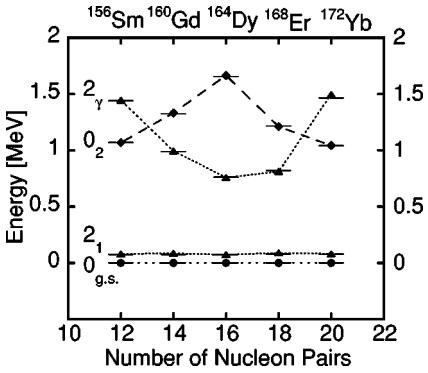

FIG. 1. The experimental and theoretical energies of the ground band $K^\pi=0^+$ and $J^\pi=2^+$ states and the nonyrast $K^\pi=0_2^+$ and $K^\pi=2_\gamma^+$ states of deformed nuclei with $F_0=0$. The experimental values [12] are indicated with bars and the calculated numbers with shapes.

jection $F_0=\frac{1}{2}(N_\pi-N_\nu)$ of the F spin. This yields a simultaneous classification of the nuclei in terms of the operators $N_\pi=\frac{1}{2}(N_p-N_p^1)$ and $N_\nu=\frac{1}{2}(N_n-N_n^1)$ which are the proton and neutron valence boson (pairs of nucleons) numbers within a given shell beyond their respective closed cores (the usual magic numbers are denoted here by N_p^1 and N_n^1). The ordering of the nuclides within this scheme can be obtained by considering sequences of nuclei with increasing total number of valence bosons N and fixed value of the difference F_0.

In this article we investigate the behavior of the 2^+ state of the g.s.b., the first excited 0_2^+ state and the 2_γ^+ bandhead configuration, which is not necessary the second 2^+ state in the $F_0=0$ multiplet of the shell, with the number of protons lying between 50 and 82, and the number of neutrons between 82 and 126. The nuclei that we consider have equal numbers of valence proton and neutron pairs and therefore differ by an α-particle-like cluster within an F_0 multiplet. As observed from the experimental data [12], the behavior of these levels is quite different, not only for different shells but also within a shell and even within different F_0 multiplets within a given shell. However, as for the states in the yrast bands, similar behavior is observed in the neighboring F_0 multiplets within a given shell. The energies of the first excited nonyrast bandheads oscillate with increasing N with opposite phase. This is particularly pronounced in the middle of the shell $(10<N<22)$, where one finds well-deformed nuclei. To deduce common features, we focused our attention on the well-deformed nuclei from the lanthanide region as these nuclei present some interesting challenges [13] from a theoretical as well as from an experimental point of view [14].

The sequence of nuclei chosen to probe the characteristic behavior of the states that were considered is shown in Fig. 1. We can separate these nuclei into three groups with similar behavior within each group: (1) at the beginning of the region $\rightarrow$ ^{152}Nd, ^{156}Sm for which $E(2_\gamma^+)>E(0_2^+)$; (2) around the middle of the multiplet $\rightarrow$ ^{160}Gd, ^{164}Dy, ^{168}Er for which $E(2_\gamma^+)<E(0_2^+)$; (3) at the end of the region $\rightarrow$ ^{172}Yb, ^{176}Hf for which $E(2_\gamma^+)>E(0_2^+)$.

The g.s.b. $J^\pi=2^+$ energies for these nuclei lie on almost a straight line at $\sim$0.07 MeV. In contrast, the energies of 0_2^+ and 2_γ^+ states oscillate out of phase as a function of N. The trends in the positions of the energies of these states form a pattern that is almost symmetric with respect to the middle of the rotational region at $N=16$ for ^{164}Dy. At this point, the energy of the first excited $K^\pi=0^+$ state has its highest value and the bandhead of the γ band has its minimum value. To either side of ^{164}Dy, for ^{160}Gd and ^{168}Er, we have $E(2_\gamma^+)<E(0_2^+)$. However, away from ^{164}Dy, to the left (^{152}Nd and ^{156}Sm) and to the right (^{172}Yb, ^{176}Hf), the two nonyrast $J^\pi=0_2^+$ and $K^\pi=2_\gamma^+$ states change their ordering in energy, $E(2_\gamma^+)>E(0_2^+)$. Three loops are formed by the lines connecting the energies of these states. The first and third loops are quite similar. Our aim is to understand and reproduce this behavior, which has many different model interpretations [1].

To understand this behavior, one must probe more deeply into the microscopic structure of these nuclei [13]. In the present work, the properties of the low-lying spectra of deformed even-even nuclei are reproduced and explained by applying a proton-neutron version of the algebraic shell model with pseudo-SU(3) symmetry [7].

III. PROTON AND NEUTRON VERSION OF THE PSEUDO-SU(3) MODEL

Elliott [15] used group-theoretical methods to investigate classification schemes for particles in a three-dimensional harmonic oscillator potential for which the underlying symmetry is SU(3). In the pseudo-SU(3) version of the model the pseudoshell $\tilde{\eta}=\eta-1$ is defined as the original "parent" shell η without its highest $j=\eta+\frac{1}{2}$ "intruder" level. In the pseudoshell containing only the normal parity states the corresponding pseudo spin-orbit interaction is negligible and hence the (pseudo-) SU(3) symmetry is restored. This mapping from the η to the $\tilde{\eta}=\eta-1$ shell yields a symmetry governed reduction of the model space to a subset of SU(3) irreps that correspond to the largest (pseudo) intrinsic deformation [10].

The proton-neutron version of the pseudo-SU(3)-shell model is a microscopic theory that respects the Pauli principle, in contrast with a classification scheme where pairs of protons and neutrons are taken to behave as bosons, such as in the interacting vector boson model [16]. The proton and neutron occupancies n_σ ($\sigma=\pi$ and ν, respectively) are determined by filling Nilsson single-particle levels from below [17] with pairs of particles in each level at a fixed value for the deformation ($\beta\sim0.3$). The changes in predicted occupancies as a function of deformation are rather rare over the normal range of deformation $\beta\sim0.25$ to $\beta\sim0.35$. Further, we consider only nucleons in normal parity orbits n_σ^+ to be spectroscopically active with those in the unique parity orbitals n_σ^- relegated to a renormalization role, an assumption that is consistent with what has been done in the past and one that is known to work well for low-lying configurations [18]. As nuclei in an $F_0=0$ multiplet have an equal number of valence protons and neutrons, the classification number N is equal to the number of valence particles of each kind. It is important to notice, however, that the protons and neutrons fill two different shells $\tilde{\eta}_\pi=3$ and $\tilde{\eta}_\nu=4$, respectively, so we have different leading SU(3) irreps for protons and neutrons

TABLE I. Occupation numbers for members of the $F_0=0$ multiplet. These numbers are used to determine the SU(3) basis states. The leading proton, neutron and coupled SU(3) quantum numbers are given in the last three columns.

Nucleus	N	n_ν	n_ν^+	n_ν^-	n_π	n_π^+	n_π^-	(λ,μ)	(λ_π,μ_π)	(λ_ν,μ_ν)
^{152}Nd	10	10	6	4	10	6	4	(30,0)	(12,0)	(18,0)
^{156}Sm	12	12	6	6	12	6	6	(30,0)	(12,0)	(18,0)
^{160}Gd	14	14	8	6	14	8	6	(28,8)	(10,4)	(18,4)
^{164}Dy	16	16	10	6	16	10	6	(30,8)	(10,4)	(20,4)
^{168}Er	18	18	10	8	18	10	8	(30,8)	(10,4)	(20,4)
^{172}Yb	20	20	12	8	20	12	8	(36,0)	(12,0)	(24,0)
^{176}Hf	22	22	14	8	22	14	8	(8,30)	(0,12)	(8,18)

with largest $C_2=(\lambda+\mu)(\lambda+\mu+3)-\lambda\mu$ values. The quadrupole-quadrupole QQ interaction, as part of the SU(3) second order invariant operator $[\tilde{C}_2=(\tilde{Q}\tilde{Q}-3\tilde{L}^2)$ with $\tilde{Q}=\tilde{Q}^\pi+\tilde{Q}^\nu$ and $\tilde{L}=\tilde{L}^\pi+\tilde{L}^\nu]$, gives preference to the "stretched" coupled representation $(\lambda,\mu)=(\lambda_\pi+\lambda_\nu,\mu_\pi+\mu_\nu)$, but in order to describe the rich and complex structure of the spectrum we need to include at least five to six additional proton and neutron pseudo-SU(3) irreps and these are also selected according to their C_2 values, with the largest being the most important. This gives rise to a large space of product representations, so they are further truncated in the same way (largest C_2 values) to a total of about 20 coupled irreps of SU(3). In Table I we give, for the nuclei considered here, the partition of the valence protons and neutrons into normal $(^+)$ and unique $(^-)$ parity orbits along with the leading SU(3) irreps only (more are included in the calculations) for nucleons in the normal parity orbits. Since we consider only even-even nuclei, only configurations with pseudospin equal to zero are taken into account [8,10].

The development of a computer code that can be used to calculate reduced matrix elements of physical operators between different SU(3) irreps [19] makes possible to include collective interactions that break the SU(3) symmetry. The importance of pairing modes in the middle of the deformed region has been pointed out in studies of the $K^\pi=0^+$ states [20], hence these terms are included in our model Hamiltonian. The Hamiltonian that is appropriate for the description of the nuclei being considered includes spherical single-particle terms for both protons and neutrons $H^\sigma_{\rm SP}$; proton and neutron pairing terms H^σ_P; an isoscalar quadrupole-quadrupole interaction QQ; and four smaller "rotorlike" terms that preserve the pseudo-SU(3) symmetry:

$$H = H^\pi_{\rm SP} + H^\nu_{\rm SP} - G_\pi H^\pi_P - G_\nu H^\nu_P - \tfrac{1}{2}\chi Q\cdot Q + aJ^2 + bK^2_J + a_3C_3 + a_sC_2, \quad (1)$$

where C_2 and C_3 are the second and third order invariants of SU(3), which are related to the axial and triaxial deformation of the nucleus. The calculations assumed standard values for the proton and neutron single-particle energies and fixed values [21] for pairing $(G_\pi=21/A, G_\nu=17/A)$, as well as for the quadrupole-quadrupole interaction strength $(\chi=35A^{-5/3})$. The other interaction strengths were varied to give a best fit to the second 0^+ (β bandhead), first 2^+ and 2^+_γ states [21]. The term proportional to K^2_J breaks the SU(3) degeneracy of the different K bands [22], the J^2 term represents a small correction to fine tune the moment of inertia, and the last term C_2, is introduced to distinguish between SU(3) irreps with λ and μ both even from the others with one or both odd [23]. The fitting was done in the following way: the interaction strengths of C_3, a_3 and C_2, a_s were varied to fit the energy of the second 0^+ state. The interaction strength b of K^2_J was varied to fit the energy of the 2^+_γ bandhead, which is not necessary the second 2^+ state. The interaction strength a of the J^2 was varied—but only slightly—to give a best fit to

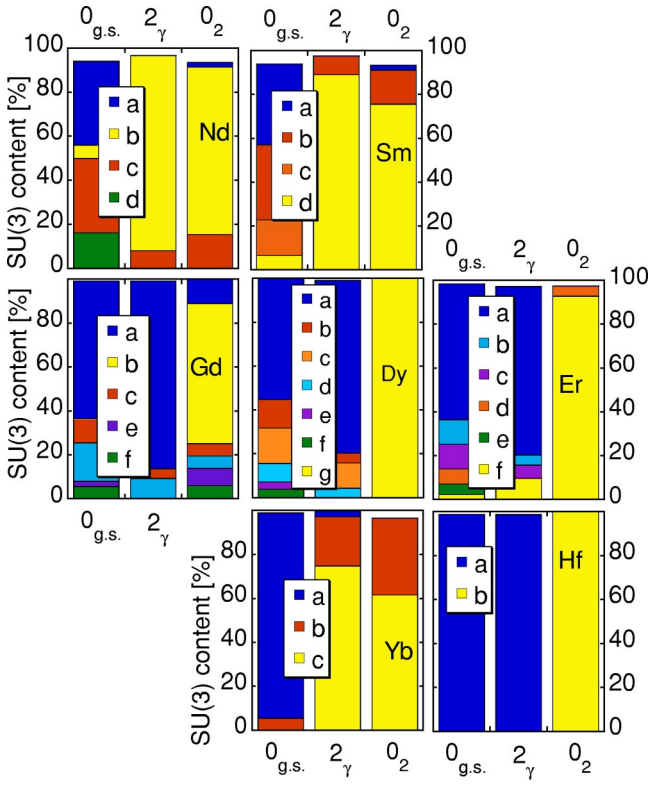

FIG. 2. (Color online) SU(3) content [%] of wave functions of the collective ground, $K^\pi=0^+_2$, and $K^\pi=2^+$ states in ^{148}Nd (upper left), ^{156}Sm (upper right), ^{160}Gd (middle left), ^{164}Dy (middle), ^{168}Er (middle right), ^{172}Yb (lower left), and ^{176}Hf (lower right). The different patterns label the SU(3) irreps given in Table II.

TABLE II. SU(3) content [%] of the ground state and $K^\pi=2^+$ and $K^\pi=0_2^+$ states in the seven nuclei shown in Fig. 2. All the basis states that contribute more than 2% are identified.

Nucleus	State	$(\lambda_\pi,\mu_\pi)\otimes(\lambda_\nu,\mu_\nu)\rightarrow(\lambda\mu)$	$0_{\text{g.s.}}$	2_γ^+	0_2^+
^{152}Nd	a	$(12,0)\otimes(18,0)\rightarrow(30,0)$	38.0		2.2
	b	$(12,0)\otimes(12,6)\rightarrow(24,6)$	6.1	88.6	75.9
	c	$(12,0)\otimes(14,2)\rightarrow(26,2)$	33.7	8.1	15.5
	d	$(8,2)\otimes(18,0)\rightarrow(26,2)$	16.2		
^{156}Sm	a	$(12,0)\otimes(18,0)\rightarrow(30,0)$	37.0		2.3
	b	$(12,0)\otimes(14,2)\rightarrow(26,2)$	34.2	8.6	15.5
	c	$(8,2)\otimes(18,0)\rightarrow(26,2)$	16.3		
	d	$(12,0)\otimes(12,6)\rightarrow(24,6)$	6.5	89.1	75.6
^{160}Gd	a	$(10,4)\otimes(18,4)\rightarrow(28,8)$	62.7	85.5	11.1
	b	$(10,4)\otimes(18,4)\rightarrow(30,4)$			63.7
	c	$(10,4)\otimes(20,0)\rightarrow(30,4)$	11.0	4.4	5.6
	d	$(12,0)\otimes(18,4)\rightarrow(30,4)$	17.5	9.3	5.6
	e	$(10,4)\otimes(18,4)\rightarrow(32,0)$	2.4		7.9
	f	$(12,0)\otimes(20,0)\rightarrow(32,0)$	5.6		6.0
^{164}Dy	a	$(10,4)\otimes(20,4)\rightarrow(30,8)$	55.3	78.8	
	b	$(10,4)\otimes(20,4)\rightarrow(32,4)$	8.4	4.3	
	c	$(10,4)\otimes(22,0)\rightarrow(32,4)$	12.9	4.4	
	d	$(12,0)\otimes(20,4)\rightarrow(32,4)$	16.2	11.6	
	e	$(10,4)\otimes(20,4)\rightarrow(34,0)$	3.3		
	f	$(12,0)\otimes(22,0)\rightarrow(34,0)$	3.9		
	g	$(10,4)\otimes(14,10)\rightarrow(24,14)$			100.0
^{168}Er	a	$(10,4)\otimes(20,4)\rightarrow(30,8)$	62.0	76.9	
	b	$(10,4)\otimes(20,4)\rightarrow(32,4)$	11.2	4.6	
	c	$(12,0)\otimes(20,4)\rightarrow(32,4)$	11.3	6.0	
	d	$(10,4)\otimes(22,0)\rightarrow(32,4)$	6.8		4.8
	e	$(10,4)\otimes(20,4)\rightarrow(34,0)$	4.8		
	f	$(10,4)\otimes(14,10)\rightarrow(24,14)$	2.3	9.7	92.7
^{172}Yb	a	$(12,0)\otimes(24,0)\rightarrow(36,0)$	93.5		2.6
	b	$(12,0)\otimes(16,10)\rightarrow(28,10)$	5.4	35.0	22.3
	c	$(4,10)\otimes(16,10)\rightarrow(20,20)$		61.6	74.8
^{176}Hf	a	$(0,12)\otimes(8,18)\rightarrow(8,30)$	98.7	98.6	
	b	$(3,9)\otimes(11,15)\rightarrow(14,24)$			100.0

the moment of inertia of the g.s.b.. Within this framework, the splitting and mixing of the pseudo-SU(3) irreps is generated by the proton and neutron single particle terms ($H_{\text{SP}}^{\pi/\nu}$) and the pairing interactions. As will be seen in the following analysis, this mixing plays an important role in the reproduction of the behavior of the low-lying collective states in the deformed nuclei.

IV. RESULTS AND DISCUSSION

A microscopic interpretation of the relative position of a collective band, as well as that of the levels within the band, follows from an evaluation of the primary SU(3) content of the collective state. A connection between the microscopic quantum numbers (λ,μ) and the collective shape variables (β,γ) is well known [11]. Our results show that if the leading configuration supports triaxiality ($\mu\neq 0$, with the triaxiality reaching a maximum when $\mu\approx\lambda$), the ground and γ bands belong to the same SU(3) irrep; if the leading SU(3) configuration is prolate ($\mu=0$), the $K^\pi=0_2^+$ and $K^\pi=2_\gamma^+$ have similar SU(3) structures. The levels within a given band have very similar content. Results are presented in Fig. 2 and Table II. All of the SU(3) product configurations that contribute more than 2% to the total are identified. An analysis of the wave functions follows.

In the first region, the bands considered for the nuclei ^{152}Nd and ^{156}Sm, have a very similar SU(3) content. The ground states are spread over almost all of the SU(3) irreps considered in the calculations with a maximum, but less than 40%, in the most symmetric leading $(12,0)\otimes(18,0)\rightarrow(30,0)$ configuration (see Table II). The $K^\pi=0_2^+$ and γ bandheads are strongly mixed, with about 89% from the γ band in the coupled $(12,0)\otimes(12,6)\rightarrow(24,6)$ configuration

TABLE III. Interaction strengths (coef) determined by fitting calculated eigenenergies to the experimental numbers for the nuclei (nucl) considered in the analysis.

coef/nucl	^{152}Nd	^{156}Sm	^{160}Gd	^{164}Dy	^{168}Er	^{172}Yb	^{176}Hf
$a_3 \times 10^{-4}$	2.57	2.59	1.93	0.65	0.75	0.31	0.43
a	0.000	0.000	0.001	−0.001	−0.002	−0.001	−0.007
b	0.00	0.55	0.153	0.042	0.022	0.12	0.3
a_s	0.000	0.000	0.004	0.001	0.001	0.001	0.006

(see Table II). In this case the bandhead of the γ band is above the bandhead of the $K^\pi=0_2^+$ band. For the ^{152}Nd nucleus, a state of angular momentum $J^\pi=2^+$, $K^\pi=2^+$ is not known experimentally. Our results predict, with an uncertainty that can be deduced by comparing theory with experiment for other states, that such a state should exist at about 1.31 MeV. This value agrees with that of the other $J^\pi=2^+$, $K^\pi=2^+$ states that are bandheads of the γ band for the considered sequence of nuclei.

For the three nuclei in the middle of the shell (^{160}Gd, ^{164}Dy, and ^{168}Er), the bandhead of the γ band lies below the bandhead of the $K^\pi=0_2^+$ band. The leading SU(3) irreps for these nuclei have quantum numbers $\mu>0$ and $\lambda>\mu$. Figure 2 shows the calculated SU(3) content for the bandheads in ^{160}Gd, ^{164}Dy, and ^{168}Er. Members of the g.s.b. and the γ band are rather strongly mixed with the largest single irrep percentage in states of the γ band. The $K^\pi=0_2^+$ band is primarily other SU(3) product configurations. For the ^{164}Dy case, where the bandhead of the γ band reaches its highest energy value there is no mixing, that is, the bandhead is 100% in $(10,4)\otimes(14,10)\rightarrow(24,14)$. Note that this is also when μ reaches its largest value.

In the third region, the experimental situation is very similar to that of the first region. However there are some important differences.

(i) The ground state for the ^{172}Yb nucleus is almost 100% $(12,0)\otimes(24,0)\rightarrow(36,0)$ with a small admixture of $(12,0)\otimes(16,10)\rightarrow(28,10)$, a configuration that plays an important, but not dominant role in the γ and $K^\pi=0_2^+$ bandhead configurations. The γ band shows the greatest amount of mixing with the 0_2^+ but with the largest percentage ($\approx$62%) in the triaxial irrep $(4,10)\otimes(16,10)\rightarrow(20,20)$.

(ii) In the case of ^{176}Hf, the protons and the neutrons in the normal parity states fill more than half the shell. This means that the SU(3) quantum numbers for the leading proton (0, 12) and neutron (8, 18) irreps have $\lambda<\mu$, which correspond to oblate intrinsic shapes and as a result the SU(3) quantum numbers for the leading irrep (8, 30) also have $\lambda<\mu$. In this case, based on the fact that $\lambda\neq 0$ (for oblate in contrast with prolate shapes) λ and μ must be interchanged in making a determination of K bands and their L content, that is, the "new" rule for oblate configurations is the same as the "old" prolate rule but with the $(\lambda,\mu)\rightarrow(\mu,\lambda)$ interchanged. Hence, one would anticipate that the ground state and the bandhead of the γ band share the same SU(3) structure, and this is in fact what happens. But one must also recognize that the shapes are now oblate rather than prolate and this changes the excitation spectra, depending on the third order invariant $\left[C_3=\frac{1}{9}(2\lambda+\mu+3)(\lambda-\mu)(\lambda+2\mu+3)\right]$ that enters the Hamiltonian. Further, it is also important to recall that it is the size of the coefficient multiplying QQ, either directly or through the coefficient a_s multiplying C_2, that determines the magnitude with which QQ enters the theory and in the case of ^{176}Hf the a_s parameter is somewhat larger and as it is used to adjust the position of the $K=0_2$ and γ bandheads in a way similar to that found in the first region.

The parameters of the Hamiltonian (1) that were obtained through a fitting procedure applied to all of the nuclei considered in this study, are given in Table III. A full understanding of the collective properties of the g.s.b. as well as the first excited $K^\pi=0_2^+$ and the 2_γ^+ bands must take into account the mixing of nonleading SU(3) configurations into their states, mixing that is driven by the Hamiltonian (1). For example, the single particle terms and the pairing interactions split and mix SU(3) irreps [24], and since the mixing normally draws in states with larger μ values the net effect of pairing is to reduce the axial deformation of the system by pulling in configurations that display greater triaxiality. (This is consistent with the notion that claims pairing drives a system towards a spherical shape.) The quadrupole-quadrupole interaction drives the proton and neutron systems towards prolate shapes if the oscillator shell is less than half full, towards oblate shapes if the respective shell is more than half full, and to large β values at maximum asymmetry for shells which are roughly half full. In addition to the quadrupole-quadrupole (χ) and the pairing strengths (G_π and G_ν) which change very smoothly as a function of mass, the "fine-tuning" of the energies of the nonyrast band states required the use of the other four parameters a_3, a, b, and a_s, which were sufficient to determine the correct behavior of the states under consideration and differences in energies of the nuclei with equivalent configurations. The latter applies to the cases of ^{152}Nd, ^{156}Sm and ^{164}Dy, ^{168}Er (see Table I). The equivalence of their corresponding SU(3) configurations is a result of the fact that the current version of the model focuses only on the particles in the normal parity orbits. The nuclei with the same SU(3) leading irreps (see Table I) differ by the number of particles in the unique parity states of the Nilsson scheme. With the interaction strengths given in Table III, the theoretical spectra of the nuclei considered are in good agreement with one another (systematic changes in interaction strengths as a function of mass) and with the experimental data, not only for bandhead configurations that we focused on here, but also for the excited states within those bands. As an example, the low lying spectra for the nucleus ^{160}Gd is presented in Fig. 3.

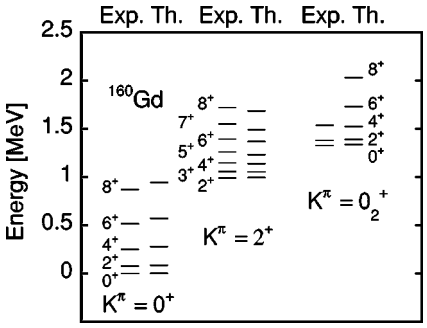

FIG. 3. Experimental and calculated low-lying energy spectrum for ^{160}Gd.

The four parameters given in Table III that were fit to obtain a correct reproduction of the energies of the states under consideration are quite important and must be considered in conjunction with the SU(3) representations in determining the shapes of the various nuclei. For example, depending upon the sign and magnitude of a_3, which determines the strength of the third order invariant C_3 of SU(3) in the Hamiltonian, one can add to or subtract from the deformation of the system by favoring or not favoring triaxial configurations. The parameter b primarily tracks the behavior of the 2_γ^+ bandhead. The strength of the quadrupole-quadrupole interaction, which enters directly with the coefficient χ, is enhanced or moderated depending upon the sign and magnitude of a_s since apart from an additive L^2 part that alters the effective moment of inertia of the system, the second order invariant C_2 of SU(3) is just QQ.

V. CONCLUSIONS

Algebraic models have emerged as a result of attempts to reproduce experimental observations with simple calculations. In the evolution of the SU(3) model, and later the pseudo-SU(3) model, one of the main motivations was to achieve a good description of deformed nuclei using a small but realistic configuration space. In the present study the configuration spaces are certainly small compared with typical ones that are used in shell-model calculations based on m-scheme configurations; nevertheless, they contain the main features of the observed complex behavior of the low-lying, nonyrast collective bands. This is a result of the microscopic basis of the theory and the fact that it correctly takes into account the distribution of particles among the single-particle levels of the valence shell. Very important to obtaining the correct results is the combination of proton and neutron representations that enter the bases states. The SU(3) coupled representations that emerge from this analysis yield information about the deformation of each system's collective states. The truncation scheme that is used is also governed by symmetry principles and tracks the onset of a deformation trough in the coupled configuration space. The Hamiltonian of the model includes terms that are not invariants of SU(3) and therefore split and mix the resultant eigenvectors. The single particle terms and the pairing interactions play an important role in determining the distribution of eigenstates across the allowed SU(3) configurations. The four parameters that are used for fine tuning the spectra permit not only a very good reproduction of the experimental data, but also give predictions as to the position of states that have not yet been experimentally identified in this region.

A microscopic interpretation of the relative position of collective bands, as well as that of the levels within these bands, follows from an evaluation of the primary SU(3) content of the collective states. The latter is closely linked to nuclear deformation [9]. In particular, a proper description of collective properties of the first excited $K^\pi = 2^+$ and $K^\pi = 0_2^+$ states must take into account the mixing of different SU(3) irreps which is driven by the Hamiltonian.

The theory can be used to predict the onset of deformation in the ground state and the low-lying, nonyrast collective bands as a function of mass number. The success of this study suggests that its applicability to other F_0 multiplets, as contained in the boson representations of the sp$(4,R)$ algebra [25], should be explored. This study also reaffirms that pseudospin zero neutron and proton configurations with a relatively few pseudo-SU(3) irreps with largest deformations (C_2 values) suffice to obtain reasonable agreement with known experimental energies of low-lying yrast and nonyrast band states in deformed nuclei (see Fig. 3). The theory simultaneously tracks changes within the bands and in the bandhead configurations themselves across a series of nuclei that differ from one another by an α-particle-like (two proton plus two neutron) clusters.

ACKNOWLEDGMENTS

Support from the U.S. National Science Foundation, Grant No. PHY-0140300, and the Southeastern Universities Research Association is gratefully acknowledged. The authors are grateful to Dr. S. L. Drenska for the help in the empirical investigation of the behavior of the nonyrast bandheads.

[1] P. E. Garrett, J. Phys. G **27**, R1 (2001).
[2] R. K. Sheline, Rev. Mod. Phys. **32**, 1 (1960).
[3] A. Bohr and B. R. Mottelson, *Nuclear Structure* (Benjamin-Cummings, Reading, MA, 1975), Vol. II.
[4] R. F. Casten, P. von Brentano, and N. V. Zamfir, Phys. Rev. C **49**, 1940 (1994).
[5] S. Drenska, A. Georgieva, V. Gueorguiev, R. Roussev, and P. Raychev, Phys. Rev. C **52**, 1853 (1995).
[6] S. Drenska, A. Georgieva, and N. Minkov, Phys. Rev. C **65**, 054303 (2002).
[7] J. P. Draayer, in *Algebraic Approaches to Nuclear Structure: Interacting Boson and Fermion Models, Contemporary Concepts in Physics VI*, edited by R. F. Casten (Harwood Academic, Chur, 1993), p. 423.

[8] J. P. Draayer and K. J. Weeks, Ann. Phys. (N.Y.) **156**, 41 (1984).
[9] T. Beuschel, J. G. Hirsch, and J. P. Draayer, Phys. Rev. C **61**, 054307 (2000).
[10] C. Vargas, J. G. Hirsch, P. O. Hess, and J. P. Draayer, Phys. Rev. C **58**, 1488 (1998).
[11] Y. Leshber and J. P. Draayer, Phys. Lett. B **190**, 1 (1987); O. Castanos, J. P. Draayer, and Y. Leshber, Z. Phys. A **329**, 33 (1988).
[12] P. C. Sood, D. M. Headly, and R. K. Sheline, At. Data Nucl. Data Tables **47**, 89 (1991); http://www.nndc.bnl.gov
[13] D. G. Burke and P. C. Sood, Phys. Rev. C **51**, 3525 (1995).
[14] A. Aprahamian *et al.*, Phys. Rev. C **65**, 031301 (2002).
[15] J. P. Elliott, Proc. R. Soc. London, Ser. A **245**, 128 (1958); **245**, 562 (1958).
[16] F. Iachello and A. Arima, *The Interacting Boson Model* (Cambridge University Press, Cambridge, 1978).
[17] S. G. Nilsson, K. Dan. Vidensk. Selsk. Mat. Fys. Medd. **29**, No. 16, 1 (1955).
[18] J. Escher, J. P. Draayer, and A. Faessler, Nucl. Phys. **A586**, 73 (1995).
[19] C. Bahri and J. P. Draayer, Comput. Phys. Commun. **83**, 59 (1994).
[20] O. Mikoshiba, R. Sheline, T. Udagava, and Shiro Yoshida, Nucl. Phys. **A101**, 202 (1967).
[21] G. Popa, J. G. Hirsch, and J. P. Draayer, Phys. Rev. C **62**, 064313 (2000).
[22] H. A. Naqvi and J. P. Draayer, Nucl. Phys. **A516**, 351 (1990); **A536**, 297 (1992).
[23] Y. Leschber, Hadronic J. Suppl. **3**, 1 (1987).
[24] C. Bahri, J. Escher and J. P. Draayer, Nucl. Phys. **A592**, 171 (1995).
[25] A. Georgieva, M. Ivanov, P. Raychev, and R. Roussev, Int. J. Theor. Phys. **25**, 1181 (1985).